Original Article
Identification of candidate targets for the diagnosis and treatment of atherosclerosis by bioinformatics analysis

Yan Gu[1*], Xiao Ma[2*], Jing Li[1], Yuhong Ma[1], Yun Zhang[1]

[1]Affiliated Hospital of Inner Mongolia Medical University, Hohhot 010050, The Inner Mongolia Autonomous Region, P. R. China; [2]Chinese People's Liberation Army No. 969 Hospital, Hohhot 010051, The Inner Mongolia Autonomous Region, P. R. China. *Co-first authors.

Abstract: Atherosclerosis, a chronic inflammatory disease, is the primary cause of most cardiovascular diseases. Circular RNAs (circRNAs) were reported to serve as post-transcriptional regulators and diagnostic markers in various diseases, but the underlying correlation between circRNAs and atherosclerosis remains elusive. In this study, we downloaded the microarray dataset GSE107522 from the Gene Expression Omnibus (GEO) and identified nine differentially expressed circRNAs (DECs). DECs expression in exosomes were investigated, and hsa_circ_0005699 was selected for subsequent analysis. We then identified 14 RNA-binding proteins (RBPs) and 71 possible hsa_circ_0005699-interacting microRNAs. Subsequently, target gene prediction and enrichment analyses were performed. The enriched pathways of RBP eIF4AIII include spliceosome, cell cycle, and pathways in cancer. We constructed a protein-protein interaction network, and 20 hub genes were identified using Search Tool for the Retrieval of Interacting Genes/Proteins and Cytoscape. Hub gene analysis revealed significant enrichment in mRNA splicing via the spliceosome, RNA splicing, protein binding, neurotrophin signaling pathway, and Ras signaling pathway. Using DrugMatrix of the Enrichr database, we identified 16 most significant small-molecule compounds that interacted with hub genes. Finally, seven hub genes (NEDD4L, FBXO44, FBXO27, WSB1, FBXW8, UBE2F, and ASB1) in cluster 1 were considered key targets associated with atherosclerosis according to MCODE analysis and the intersection between the module and hub genes. Thus, hsa_circ_0005699, RBP eIF4AIII, and the seven identified hub genes (NEDD4L, FBXO44, FBXO27, WSB1, FBXW8, UBE2F, and ASB1) could help to elucidate the pathogenesis and progression of atherosclerosis. This work may contribute to providing candidate targets for the diagnosis and treatment of atherosclerosis.

Keywords: Atherosclerosis, circRNA, diagnosis, biomarker, treatment

Introduction

Cardiovascular disease (CVD) produces immense health and economic burdens worldwide, causing approximately 17 million deaths per year [1]. The prevalence of CVD increases with advancing age in both men and women. Atherosclerosis, a chronic inflammatory disease, is the major cause of CVD, including myocardial infarction, heart failure, and stroke [2]. The pathogenesis of atherosclerosis comprises a series of steps, including endothelial dysfunction, fatty-streak formation, fibrous cap formation, and plaque instability and rupture [3]. Oxidized low-density lipoprotein (oxLDL) may promote the development of atherosclerosis by inducing the adhesion of monocytes to

the arterial intima and stimulating the differentiation of endometrial monocytes into resident macrophages [4]. Therefore, the identification of reliable biomarkers related to atherosclerosis has clinical and theoretical significance.

Circular RNAs (circRNAs) are covalently closed, single-stranded transcripts [5], which have been classified as non-coding RNAs with potential as post-transcriptional regulators and diagnostic markers [6-8]. Numerous recent studies have shown that many circRNAs have biological functions and their dysregulated expression is associated with complicated diseases, such as hepatocellular carcinoma [9], breast cancer [10], and heart failure [11]. Despite the numerous identified circRNAs in
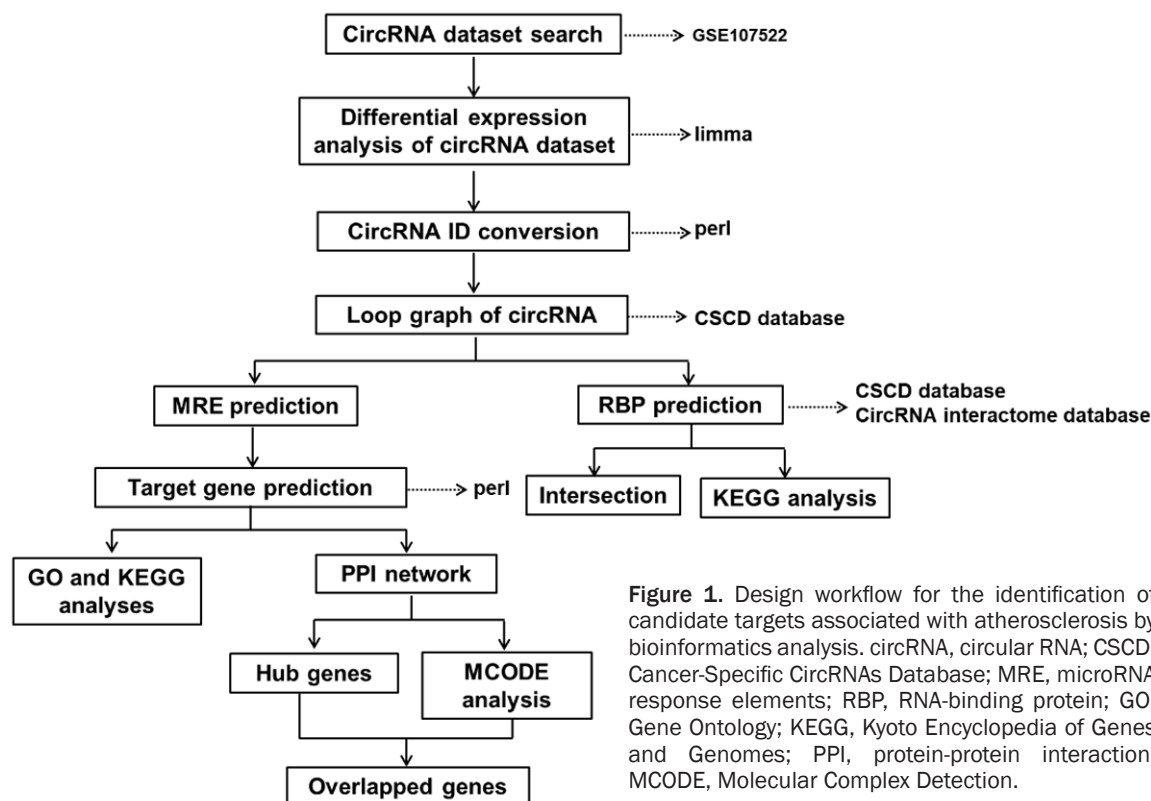
Figure 1. Design workflow for the identification of candidate targets associated with atherosclerosis by bioinformatics analysis. circRNA, circular RNA; CSCD, Cancer-Specific CircRNAs Database; MRE, microRNA response elements; RBP, RNA-binding protein; GO, Gene Ontology; KEGG, Kyoto Encyclopedia of Genes and Genomes; PPI, protein-protein interaction; MCODE, Molecular Complex Detection.

various diseases, atherosclerosis-associated circRNAs remain to be explored.

In the past few decades, microarray technology and bioinformatics analysis have been widely used to screen genetic variation at the genomic level. In the present study, the microarray dataset GSE107522 from the Gene Expression Omnibus (GEO) database was downloaded and analyzed to obtain differentially expressed circRNAs (DECs) between oxLDL-treated macrophages and control samples. RNA-binding proteins (RBPs) and microRNA response elements (MREs) were then predicted by the Cancer-Specific CircRNAs Database (CSCD, http://gb.whu.edu.cn/CSCD/). Subsequently, Gene Ontology (GO), Kyoto Encyclopedia of Genes and Genomes (KEGG) pathway enrichment and protein-protein interaction (PPI) network analyses were performed to help to elucidate the molecular mechanisms involved in the progression of atherosclerosis. Finally, key cluster and hub genes were screened out using hub gene and molecular complex detection (MCODE) analyses. In addition, the results ROC analyses showed that those circRNAs were potential predictors of atherosclerosis. The detailed workflow for this work is depicted in **Figure 1**.

Materials and methods

Collection of clinical samples

The blood of patients with atherosclerosis and healthy people were collected from the affiliated Hospital of Inner Mongolia Medical University (Inner Mongolia, China). The clinical blood samples were collected according to established clinical protocols with informed consent from all patients. The blood samples were stored in liquid nitrogen prior to being subjected to further experiments. The protocols for collecting and using the clinical samples were approved by the Institutional Research Ethics Committee of the affiliated Hospital of Inner Mongolia Medical University (Inner Mongolia, China).

Quantitative real-time PCR (qRT-PCR)

Total RNA was extracted from plasma samples using TRIzol (Thermol Fisher Scientific, MA, USA) and reverse transcription was performed using miScript II RT Kit (Qiagen, MD, USA) and cDNA amplification using the SYBR Green Master Mix kit (Takara, Otsu, Japan). Total RNA was pretreated to enrich circRNA using Circ-

RNA Enrichment Kit (Cloud-seq Inc., USA). RNA libraries were constructed by using pretreated RNAs with TruSeq Stranded Total RNA Library Prep Kit (Illumina, San Diego, CA, USA) according to the manufacturer's instructions. Libraries were controlled for quality and quantified using the BioAnalyzer 2100 system (Agilent Technologies, Inc., USA). The libraries were denatured as single-stranded DNA molecules, captured on Illumina flow cells, amplified in situ as clusters and finally sequenced for 150 cycles on Illumina HiSeq Sequencer (USA) according to the manufacturer's instructions.

Data collection and preprocessing

The GSE107522 dataset and GPL19978 platform annotation file (Agilent-069978 Arraystar Human CircRNA microarray V1) were downloaded from the GEO [12] database (https://www.ncbi.nlm.nih.gov/geo/). By writing perl scripts to annotate the probe of the GSE107-522 expression matrix according to the platform annotation file, we obtained the circRNA expression matrix. The ID of the circRNA was then circularized to the ID in the circBase format according to the Agilent circRNA annotation file. The GSE107522 dataset contained three macrophage control samples and three oxLDL-treated macrophages samples.

Differential expression analysis

DECs were screened using |log2FC| >1 and $P<0.05$ as the screening conditions in R software with the Limma package loaded (R version 3.6.1: https://www.r-project.org/). Next, the heat map was drawn using the selected DECs using the pheatmap package. Furthermore, we retrieved DEC-related information in the circBase [13] database (http://www.circbase.org/). The expression level of DECs in exosomes was then searched in the exorbase [14] database (http://www.exorbase.org/).

Analyses of GO and KEGG enrichment

GO is an important bioinformatics tool to annotate genes and analyze the biological processes of these genes. GO analysis included biological processes (BP), cellular components (CC), and molecular functions (MF). KEGG (http://www.genome.jp/) is a systematic analysis of gene function to identify biological regulatory pathways. The official gene symbol was trans-

formed into the gene ID using the org.Hs.eg.db package. GO and KEGG pathway analyses were performed using the clusterProfiler package, and cluster analysis was performed using the GO plot package. Differences associated with $P<0.05$ and $q<0.05$ were considered significant.

Prediction and analysis of RBPs

The RBPs of DECs were predicted using the CSCD [15] (http://gb.whu.edu.cn/CSCD/) and the Circular RNA Interactome database [16] (https://circinteractome.nia.nih.gov/). Next, we obtained the intersection of RBP prediction from these two databases using the venny 2.1 online website (https://bioinfogp.cnb.csic.es/tools/venny/). KEGG pathway analysis of the RBPs shared by the two databases was then performed under the path module of the starBase [17] database (http://starbase.sysu.edu.cn/).

PPI network construction of target genes

The MREs of DECs were predicted using the CSCD (http://gb.whu.edu.cn/CSCD/). The MRE target gene prediction files were then downloaded from the miRDB [18] database (http://www.mirdb.org/), miRTarbase [19] database (http://mirtarbase.mbc.nctu.edu.tw/php/index.php) and TargetScan (http://www.targetscan.org/vert_72/). Using perl script, we obtained the target genes predicted by all three databases. The PPI network of the target genes was constructed using the STRING [20] database (https://string-db.org/), and interactions with a combined score greater than 0.9 were considered to be statistically significant. The PPI network was drawn using the Network Analyzer plug-in of Cytoscape [21], an open-source bioinformatics software program to visualize molecular interaction networks.

Hub gene selection and analysis

CytoHubba [22] is a Cytoscape plug-in to explore PPI network hub genes. We screened the top 20 hub genes by the degree method in CytoHubba. The redder color represents a greater gene degree. The function of the hub genes was then analyzed using the DAVID [23] online database (https://david.ncifcrf.gov/summary.jsp). Small-molecule compounds that can interact with hub genes were predicted by

DrugMatrix analysis in the Enrichr [24] online database (http://amp.pharm.mssm.edu/Enrichr/). Additionally, *P*<0.05 was set as the screening standard.

MCODE analysis

As reported previously, MCODE is a useful tool that is widely used to assess densely connected regions in large PPI networks probably involved in molecular complexes [25]. Thus, MCODE was used to identify the core protein complex in the PPI network constructed in this work. Briefly, the PPT network obtained by STRING was analyzed using the MCODE plug-in of Cytoscape. The parameters were set as follows: degree cutoff =2; cluster finding = haircut; node score cutoff =0.2; K-score =4; maximum depth =100.

Statistical analysis

All the data were subjected to statistical analysis by using SPSS 24.0 and GraphPad Prism 7. The results were tested for variance normality and homogeneity. Two treatment groups were compared by the unpaired Students t test. Mann-Whitney test was used to evaluate the non-normally distributed data. Statistical difference of multiple groups determined by a one-way analysis of variance. Multivariate logistic regression analysis was applied to evaluate the relationship between cerebrovascular atherosclerosis and related risk factors. ROC was used to characterize the predictive function of distinguishing cerebral atherosclerosis from the control group, and the area under the ROC curve (AUC) was calculated to evaluate the diagnostic performance of the selected markers. The correlation coefficient analysis of Spearman is used to analyze the correlation. Kaplan-Meier method and logarithmic rank test were used to analyze the event-free curve. *P*<0.05 was considered to demonstrate statistically significant differences.

Results

Identification of DECs

After the standardization of GSE107522, we obtained 9 DECs (**Figure 2A**) and the heat map for the DECs (**Figure 2B**). Compared with the control group, eight circRNAs were up-regulat-ed and one circRNA was down-regulated in oxLDL-treated THP-1 macrophages (**Table 1**). To screen the target circRNA from these nine DECs for subsequent analysis, we retrieved information in the circBase database. We found that the gene symbols of hsa_circ_0003645 and hsa_circ_0005699 were both C16orf62 and both genes were expressed in many samples. Interestingly, by comparing the nucleic acid sequences, we found that hsa_circ_000-5699 contained the nucleic acid sequence of hsa_circ_0003645 (**Figure 2C**).

Expression level in human blood exosomes

By searching the expression level of C16orf62 in human blood exosomes in the exorbase database, we found that the expression level of this gene in exosomes ranked 20%-30%, and the gene could generate 27 circRNAs (**Figure 3A**). By further investigation of the expression levels of these 27 circRNAs in human blood exosomes, we found that hsa_circ_00-05699 ranked first and hsa_circ_0003645 ranked third (**Figure 3B**). Therefore, we chose hsa_circ_0005699 for subsequent analysis. Additionally, hsa_circ_0005699 was found to be down-regulated in the blood exosomes of patients with coronary heart disease (CHD in **Figure 3B**) and up-regulated in colorectal cancer (CRC in **Figure 3B**) patients. These results revealed that hsa_circ_0005699 might be transported by exosomes to regulate target cells.

RBP prediction and KEGG pathway analysis

Dysregulation of RBP is associated with many diseases, such as cardiomyopathy, neurological diseases, and various cancers [26]. Thus, we conducted RBP prediction of hsa_circ_0005699 in CSCD and CircRNA Interactome databases. The CSCD online database revealed 14 RBPs of hsa_circ_0005699 (**Table 2**). The CircRNA Interactome database showed that hsa_circ_0005699 only contained RBP eIF4AIII. To identify the function of eIF4AIII, KEGG pathway analysis was then performed using the starBase database. The outcome of eIF4AIII analysis revealed significant enrichment in many pathways, including Spliceosome, Cell Cycle, and Pathways in Cancer (**Table 3**).
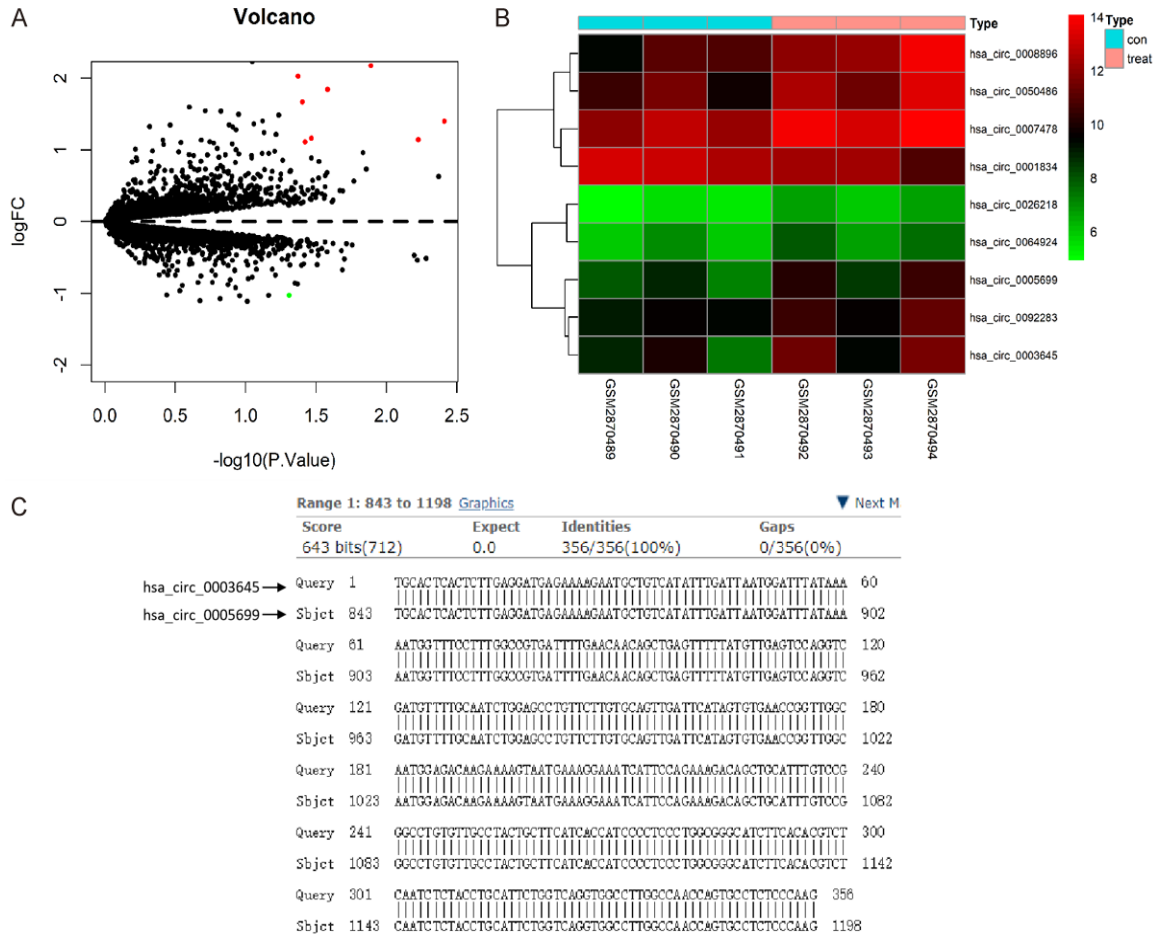
Figure 2. Identification of DECs associated with atherosclerosis in the GEO database. A. Volcano plot of detectable DECs associated with atherosclerosis from the GSE107522 dataset analyzed by R software with the limma package loaded. Red plots stand for up-regulated circRNAs, and green ones represent down-regulated circRNAs with |log2FC| >1 and P<0.05. The black plots indicate nonsignificant genes. The abscissa shows the -log10 of the adjusted *p*-value for each gene, indicating the strength of the association. The ordinate presents the FC in circulating the gene expression between the samples and control. B. Heat map of DECs as analyzed by pheatmap. C. The nucleic acid sequences of hsa_circ_0003645 and hsa_circ_0005699, derived from circBase database (http://www.circbase.org/), were compared. DECs, differentially expressed circRNAs; GEO, gene expression omnibus; FC, fold change.

Table 1. DECs in oxLDL-treated macrophages

circBase ID	Log2FC	AveExpr	P-Value
hsa_circ_0008896	2.18	11.54	0.01
hsa_circ_0003645	2.03	9.76	0.04
hsa_circ_0050486	1.84	11.51	0.03
hsa_circ_0005699	1.67	8.91	0.04
hsa_circ_0007478	1.4	13.03	0
hsa_circ_0064924	1.16	6.86	0.03
hsa_circ_0026218	1.14	5.85	0.01
hsa_circ_0092283	1.11	9.97	0.04
hsa_circ_0001834	-1.03	12.41	0.05

DECs, differentially expressed circRNAs; circRNA, circular RNA; oxLDL, oxidized low-density lipoprotein.

MRE prediction and GO and KEGG pathway analyses of targets genes for hsa_circ_0005699-associated miRNAs

By inhibiting target genes, miRNAs have been reported to play a multifaceted role in many diseases [27]. To identify miRNAs that hsa_circ_0005699 may interact with, we performed MRE analysis using the CSCD database. hsa_circ_0005699 may interact with 71 miRNAs. Based on the MRE target gene prediction files from miRDB, miRTarbase, and TargetScan, we found 616 target genes of these miRNAs that were then subjected to GO and

Figure 3. Expression levels of DECs in human blood exosomes according to the exorbase database (http://www.exorbase.org/). A. The detailed information of C16orf62 in exosomes was obtained from the exorbase database. B. The detailed information of circRNAs (mainly hsa_circ_0005699 and hsa_circ_0003645) generated by C16orf62 in exosomes was analyzed using the exorbase database. hsa_circ_0005699 ranked first, and hsa_circ_0003645 ranked third. hsa_circ_0005699 was down-regulated in the blood exosomes of patients with CHD and up-regulated in CRC patients. DECs, differentially expressed circRNAs; CHD, coronary heart disease; CRC, colorectal cancer; HCC, hepatocellular carcinoma; PAAD, pancreatic adenocarcinoma.

Table 2. RNA-binding proteins of hsa_circ_0005699 in the CSCD database

Name	Total	RNA-binding protein
hsa_circ_0005699	14	AGO1, FMRP, DGCR8, AGO2, eIF4AIII, HuR, IGF2BP3, FUS, LIN28, IGF2BP1, PTB, IGF2BP2, TDP-43, UPF1

CSCD, Cancer-Specific CircRNAs Database.

Table 3. KEGG Pathway Enrichment Analysis of eIF4AIII

Pathway Name	Log10 (FDR)
KEGG_Spliceosome	-10.07172
KEGG_Cell_Cycle	-9.44379
KEGG_Ribosome	-8.32863
KEGG_Pathways_In_Cancer	-7.61845
KEGG_Lysosome	-6.63144
KEGG_Endocytosis	-6.27261
KEGG_Pancreatic_Cancer	-6.23871
KEGG_Focal_Adhesion	-6.22948
KEGG_Mapk_Signaling_Pathway	-4.91146
KEGG_Wnt_Signaling_Pathway	-2.18551

KEGG, Kyoto Encyclopedia of Genes and Genomes.

KEGG pathway enrichment analyses. GO analysis results showed (**Figure 4A**) that changes in BP were significantly enriched in small GTPase-mediated signal transduction, covalent chromatin modification, and histone modification. Changes in CC were mainly enriched in the transcription factor complex, nuclear periphery, and transcriptional repressor complex. Changes in MF were significantly enriched in DNA-binding transcription activator activity, RNA polymerase II specific, and repressing transcription factor binding. The GO enrichment results were then clustered by cluster-Profiler package (**Figure 4B**). The KEGG pathway results showed that these target genes
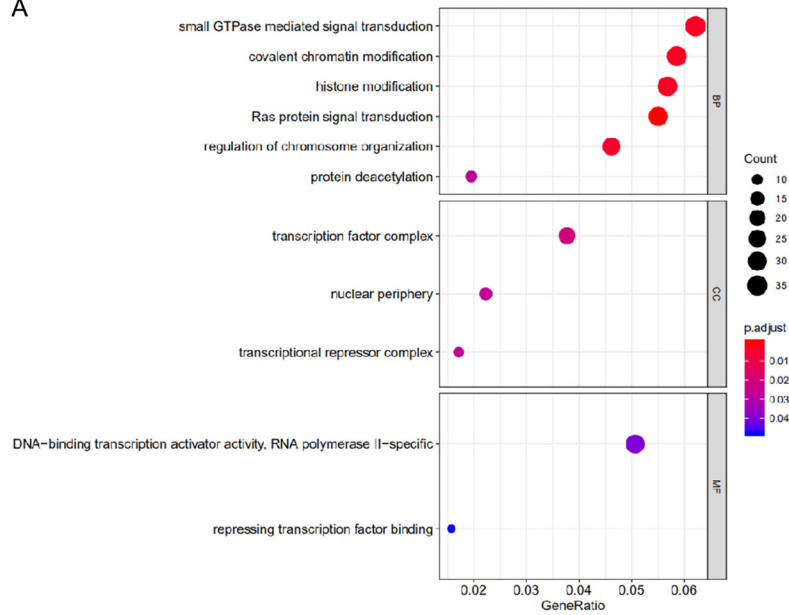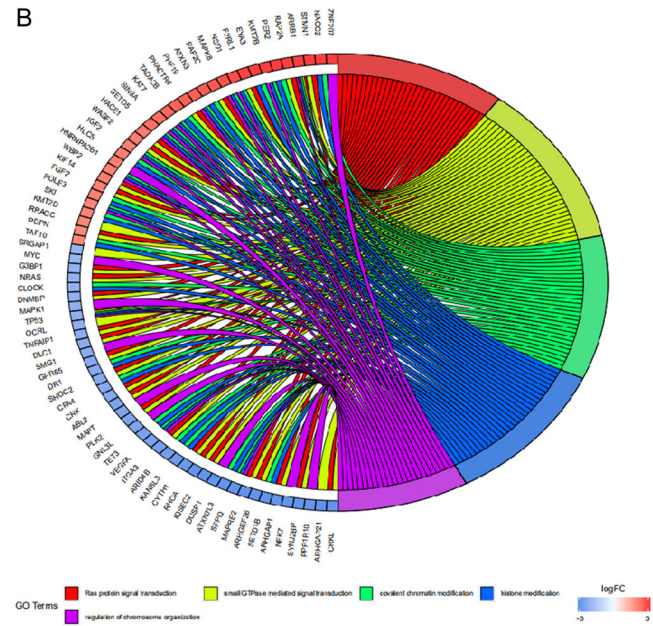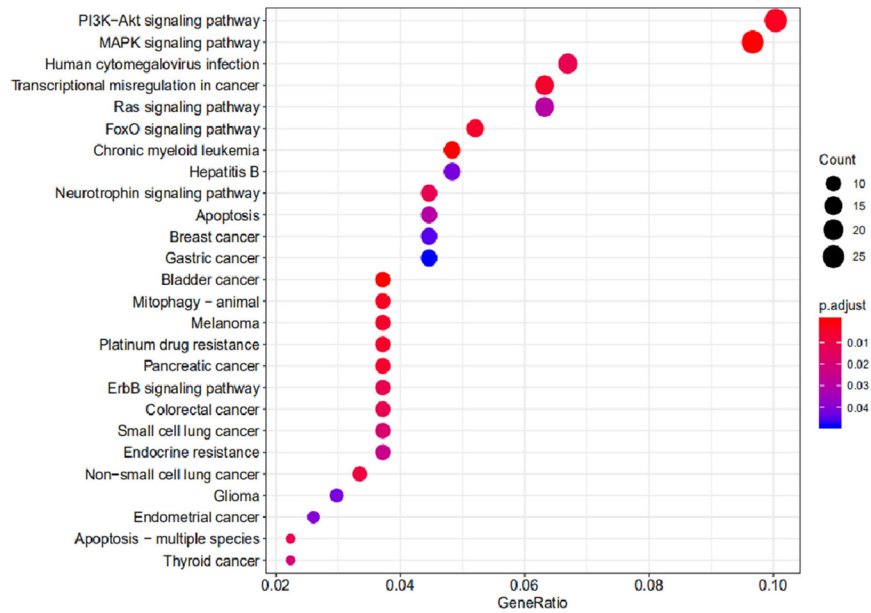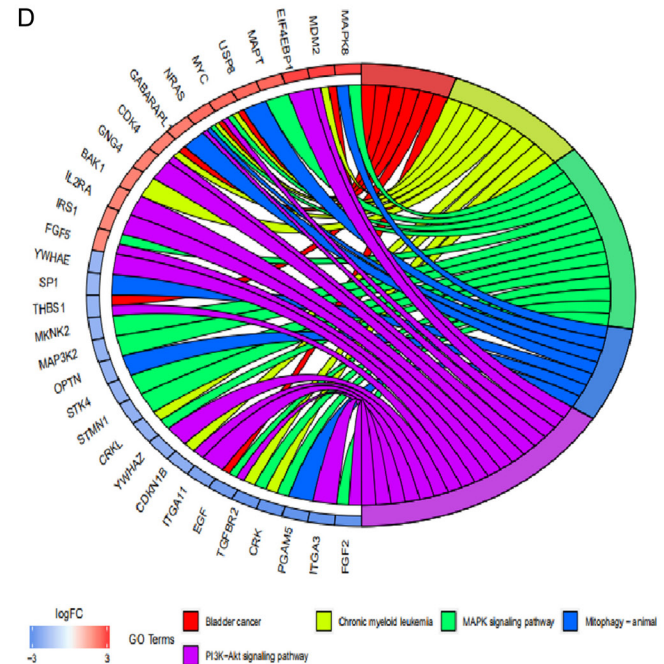
Candidate targets involved in atherosclerosis

Figure 4. GO and KEGG pathway analyses of target genes for hsa_circ_0005699-associated miRNAs. A. GO enrichment analysis of target genes obtained from the clusterProfiler package. B. Clustered GO enrichment was analyzed using the GO plot package. C. KEGG pathway enrichment analysis of target genes obtained from the clusterProfiler package. These target genes were significantly enriched in the PI3K-Akt signaling pathway, MAPK signaling pathway, and FoxO signaling pathway. D. Clustered KEGG pathway enrichment was analyzed using the GOplot package. GO, Gene Ontology; KEGG, Kyoto Encyclopedia of Genes and Genomes; BP, biological processes; CC, cellular components; MF, molecular functions.

were significantly enriched in the PI3K-Akt signaling pathway, MAPK signaling pathway, and FoxO signaling pathway (**Figure 4C**). Similarly, clustering analysis was then performed on the KEGG enrichment results using the clusterProfiler package (**Figure 4D**).

Hub gene selection and analysis

To determine the hub genes among the target genes, the PPI network of target genes was constructed using the STRING database (**Figure 5A**), followed by analysis using Cytoscape software. Subsequently, using the degree method of CytoHubba, the top 20 genes were identified as hub genes (**Figure 5B**). The top-20 hub genes are listed in **Table 4**. To determine the function of these hub genes, we performed GO and KEGG enrichment analyses in the DAVID database. These 20 hub genes were mainly enriched in mRNA splicing, via the spliceosome, RNA splicing, protein binding, neurotrophin signaling pathway, and Ras signaling pathway (**Table 5**). Finally, using DrugMatrix of the Enrichr database, we found the 16 most significant small-molecule compounds that can interact with these hub genes, such as methapyrilene, stavudine, and loratadine (**Table 6**).

MCODE analysis and overlapped genes

Based on the PPI network constructed above, the network clusters were subsequently analyzed using the MCODE plug-in software. According to the operating conditions described in the Materials and methods section, four clusters were obtained (**Figure 6**). Subsequently, the genes previously generated in these four clusters and hub genes were overlapped to further screen out the most vital cluster. As indicated in **Table 7**, the common genes in cluster 1 and the top-20 hub genes included NEDD4L, FBXO44, FBXO27, WSB1, FBXW8, UBE2F, and ASB1, accounting for 35% in cluster 1. The common genes in cluster 2 and the top-20 hub genes included RNPS1, CDC5L, SNRPB, U2AF2, GTF2F1, and SRSF2, account-

ing for 30% in cluster 2. The common genes in cluster 4 and the top-20 hub genes included NRAS, MAPK1, TNRC6A, and RHOA, accounting for 8% in cluster 4. However, no intersection was found between cluster 3 and the top-20 hub genes. Accordingly, seven hub genes in cluster 1-NEDD4L, FBXO44, FBXO27, WSB1, FBXW8, UBE2F, and ASB1-were considered the key targets associated with atherosclerosis.

The expression of hsa_circ_0005699 expression in plasma and low-density lipoprotein cholesterol (LDL-C) level with cerebral atherosclerosis

To further confirm the role of hsa_circ_0005699 in the involvements of CVDs, we investigated the expression levels of hsa_circ_0005699 in the plasma samples from healthy control and patients with atherosclerosis. The qRT-PCR results showed that hsa_circ_0005699 expression levels were up-regulated in the plasma isolated from atherosclerotic patients compared to heathy controls (**Figure 7A**, P=0.0015), and hsa_circ_0005699 expression in the plasma was positively related with cerebral atherosclerosis and LDL-C level (**Figure 7B**, r=0.08651, P=0.0135). Subsequent ROC analysis was adopted to predict the impact of hsa_circ_0005699 in the plasma and LDL-C level on cerebral atherosclerosis. The AUC of hsa_circ_0005699 in the plasma was 0.723 (95% CI 0.6068-0.8393, P=0.0033) (**Figure 7C**) and the AUC of LDL-C level was 0.723 (95% CI 0.6068-0.8393, P=0.0033) (**Figure 7D**). Interestingly, the AUC of the combination of hsa_circ_0005699 in the plasma and LDL-C level was 0.723 (95% CI 0.6068-0.8393, P=0.0033) (**Figure 7E**). These results indicated that the combination of hsa_circ_0005699 and LDL-C had more effectively than either hsa_circ_0005699 or LDL-C alone.

Discussion

Atherosclerosis, induced by chronic inflammation and perturbed by lipid accumulation, is

Candidate targets involved in atherosclerosis
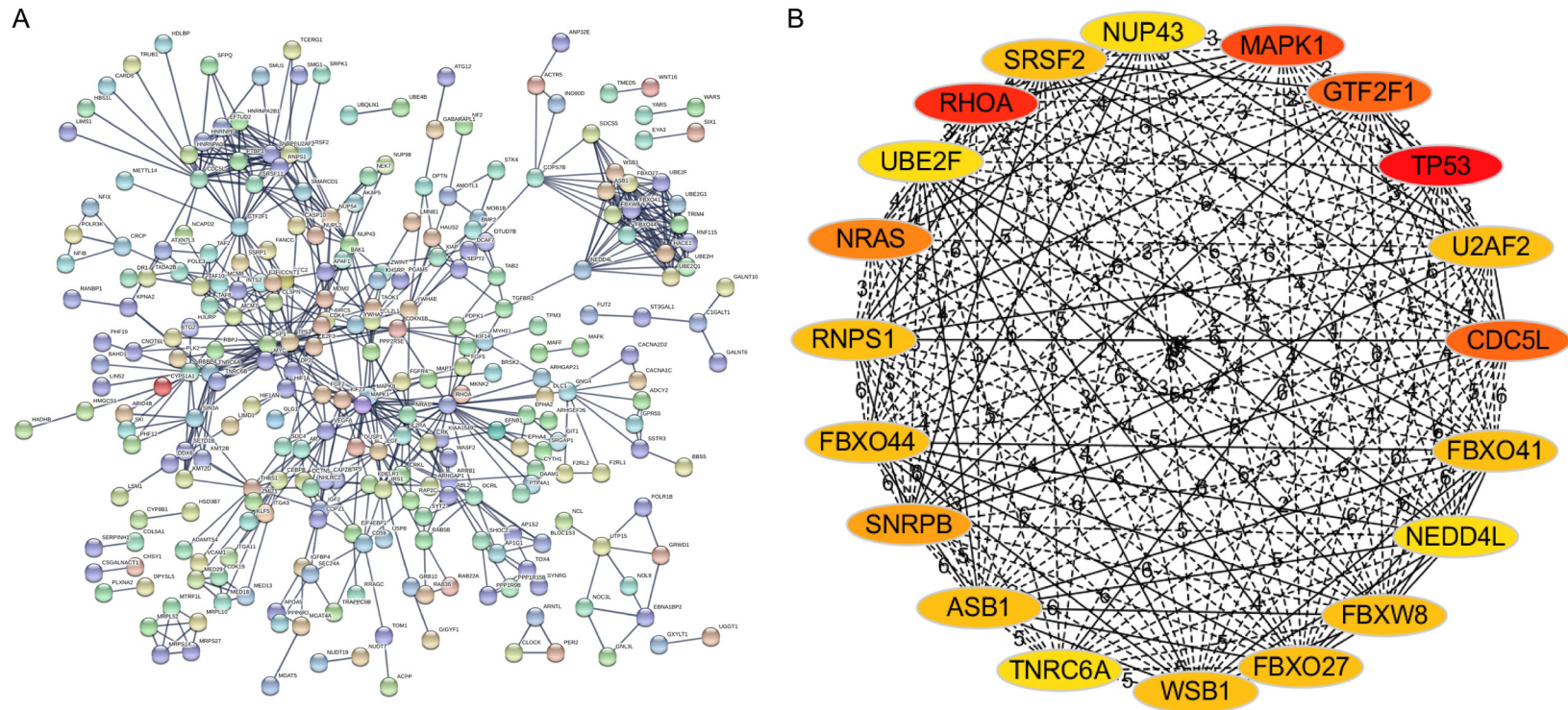
Figure 5. PPI networks of target genes and hub gene selection. A. The PPI networks of target genes were constructed based on the STRING database (http://string-db.org). B. The top-20 hub genes were identified according to the degree method of CytoHubba. PPI, protein-protein interaction; STRING, Search Tool for the Retrieval of Interacting Genes.

Table 4. List of the top-20 hub genes

Total	Hub gene name
20	NUP43, MAPK1, GTF2F1, TP53, U2AF2, CDC5L, FBXO41, NEDD4L, FBXW8, FBXO27, WSB1, TNRC6A, ASB1, SNRPB, FBXO44, RNPS1, NRAS, UBE2F, RHOA, SRSF2

Table 5. GO and KEGG pathway enrichment analyses of the hub genes

Category	Term	Count	P-Value
GOTERM_BP_DIRECT	GO: 0000398~mRNA splicing, via spliceosome	6	0.00
GOTERM_BP_DIRECT	GO: 0006406~mRNA export from nucleus	4	0.00
GOTERM_BP_DIRECT	GO: 0016032~viral process	4	0.00
GOTERM_BP_DIRECT	GO: 0016567~protein ubiquitination	4	0.00
GOTERM_BP_DIRECT	GO: 0008380~RNA splicing	3	0.01
GOTERM_CC_DIRECT	GO: 0005654~nucleoplasm	10	0.00
GOTERM_CC_DIRECT	GO: 0019005~SCF ubiquitin ligase complex	3	0.00
GOTERM_CC_DIRECT	GO: 0005681~spliceosomal complex	3	0.00
GOTERM_CC_DIRECT	GO: 0005622~intracellular	6	0.01
GOTERM_MF_DIRECT	GO: 0005515~protein binding	17	0.00
GOTERM_MF_DIRECT	GO: 0000166~nucleotide binding	4	0.00
GOTERM_MF_DIRECT	GO: 0008134~transcription factor binding	3	0.03
KEGG_PATHWAY	hsa05216: Thyroid cancer	3	0.00
KEGG_PATHWAY	hsa04722: Neurotrophin signaling pathway	4	0.00
KEGG_PATHWAY	hsa03040: Spliceosome	4	0.00
KEGG_PATHWAY	hsa05219: Bladder cancer	3	0.00
KEGG_PATHWAY	hsa05213: Endometrial cancer	3	0.00
KEGG_PATHWAY	hsa05161: Hepatitis B	3	0.03
KEGG_PATHWAY	hsa05200: Pathways in cancer	4	0.03
KEGG_PATHWAY	hsa04014: Ras signaling pathway	3	0.04
KEGG_PATHWAY	hsa04010: MAPK signaling pathway	3	0.05

Abbreviations: GO, Gene Ontology; KEGG, Kyoto Encyclopedia of Genes and Genomes; BP, biological processes; CC, cellular components; MF, molecular functions.

recognized as the primary cause of most cardiovascular diseases [28]. The initial pathology manifestation is the recruitment of monocytes into the subendothelial space and the accumulation of oxLDL to form fatty-streak lesions [29]. Recently, circRNAs have received attention in the development of various diseases. For example, Tan S et al. found a novel oncogenic circRNA F-circEA-2a that can promote cell migration and invasion in non-small cell lung cancer [30]. Hsiao KY et al. identified a group of novel circRNAs expressed in colorectal cancer, and circCCDC66 promotes colon cancer growth and metastasis by protecting multiple oncogenes from being attacked by miRNAs [31]. However, the potential circRNAs associated with the pathogenesis and development of atherosclerosis remain to be further explored.

In the present study, the microarray dataset GSE107522 was analyzed to obtain DECs between oxLDL-treated THP-1 macrophages and the control group. We found nine DECs, including eight up-regulated DECs and one down-regulated DEC. Studies have shown the value of circRNAs as potential biomarkers of CVD [8]. Therefore, these DECs may serve as potential biomarkers and therapeutic targets for atherosclerosis. Based on the analysis results from circBase and exorbase databases, hsa_circ_0005699 was chosen for subsequent analysis because it has the highest expression level in human blood exosomes. Additionally, we found that hsa_circ_0005699 is down-regulated in the blood exosomes of patients with coronary heart disease and up-regulated in colorectal cancer patients. Studies have shown that exosomal circRNAs have

Table 6. List of the most significant small-molecule compounds provided by DrugMatrix

Term	P-Value	Odds Ratio	Combined Score
Methapyrilene	7.89E-05	16.95	160.12
Stavudine	7.89E-05	16.95	160.12
L-Buthionine_Sulfoximine	1.31E-04	14.87	132.96
Loratadine	1.42E-04	14.55	128.82
Amikacin	1.77E-04	13.75	118.76
Valeric_Acid	1.82E-04	13.65	117.59
Sparteine	1.84E-04	13.61	117.01
Baclofen	1.96E-04	13.38	114.19
Maprotiline	1.99E-04	13.33	113.64
Emetine	2.01E-04	13.29	113.09
Oxaliplatin	2.12E-04	13.11	110.95
Microcystin	2.23E-04	12.94	108.87
Pantoprazole	2.25E-04	12.90	108.35
Nortriptyline	2.34E-04	12.78	106.85
Doxorubicin	2.45E-04	12.62	104.89
Chlorambucil	2.48E-04	12.58	104.41

potential applications as disease biomarkers and novel therapeutic targets [32]. Zhang X et al. proved that circNRIP1 could be transmitted by exosomal communication between gastric cancer cells, and exosomal circNRIP1 promoted tumor metastasis in vivo [33]. Therefore, we speculate that macrophages may regulate atherosclerosis progression by secreting exosomal hsa_circ_0005699.

CircRNAs mainly play their roles by competing with RBPs and miRNAs to regulate their target genes. For example, Zhu YJ et al. revealed that circZKSCAN1 suppresses cell stemness in HCC by competing against the RBP FMRP [34]. Wang K et al. identified a circRNA that can inhibit cardiac hypertrophy and heart failure by acting as an endogenous miR-223 sponge [11]. In our study, we identified 14 RBPs, especially eIF4AIII, which may compete against hsa_circ_0005699. The outcome of KEGG pathway analysis regarding eIF4AIII revealed significant enrichment in Spliceosome, Cell Cycle, and Pathways in Cancer. These results elucidated that hsa_circ_0005699 may interact with RBP eIF4AIII to regulate pathways to perform related functions.

Next, we identified 71 possible hsa_circ_0005699-interacting miRNAs and 616 target genes of MREs. Studies have reported that mRNAs, long non-coding RNAs, and circRNAs can serve as competing endogenous RNAs (ceRNAs) to regulate expression by competing for miRNA binding through shared MREs [35]. For example, Cheng Z et al. found that circTP63 shares MREs with FOXM1 and competitively binds to miR-873-3p, resulting in the promotion of lung squamous cell carcinoma progression by up-regulating FOXM1 [36]. Chen L et al. elucidated the endogenous competitive relationships among circRNA 100146, SF3B3, and miRNAs in non-small cell lung cancer, and circRNA 100146 affected tumor progression via the regulation of miR-361-3p and miR-615-5p [37]. These results indicate that hsa_circ_0005699 may exert an influence on the progression of atherosclerosis through the ceRNA mechanism.

These target genes were subjected to PPI network construction, which identified 20 hub genes. Subsequently, GO and KEGG enrichment analyses of the 20 hub genes found that they were mainly enriched in mRNA splicing, via the spliceosome, RNA splicing, protein binding, the neurotrophin signaling pathway, and the Ras signaling pathway. Furthermore, we identified 16 small-molecule compounds that can interact with the hub genes, suggesting that these small-molecule drugs, such as methapyrilene, stavudine, and loratadine, may have potential value in the treatment of atherosclerosis. Finally, MCODE and intersection analyses were performed to mine the key hub genes. Seven hub genes in cluster 1-NEDD4L, FBXO44, FBXO27, WSB1, FBXW8, UBE2F, and ASB1-were considered key targets associated with atherosclerosis. Several studies on these hub genes have been carried out in various diseases. For example, NEDD4L was reported to be associated with cardiovascular disease [38] and glioma [39]. Only one article regarding the association of FBXO44 with disease revealed that the degradation of RGS2 protein regulated by FBXO44 solely depends on a Cullin 4B/DDB1 complex, indicating a novel therapeutic approach to hypertension, anxiety, and other diseases associated with RGS2 dysregulation [40]. Regarding FBXO27 (also named SCF), several studies have outlined that it is closely related to autophagy [41, 42]. Additionally, WSB1 was shown to be involved in a few carcinomas [43, 44]. FBXW8 (also named CRL7) was reported to be associated with some can-
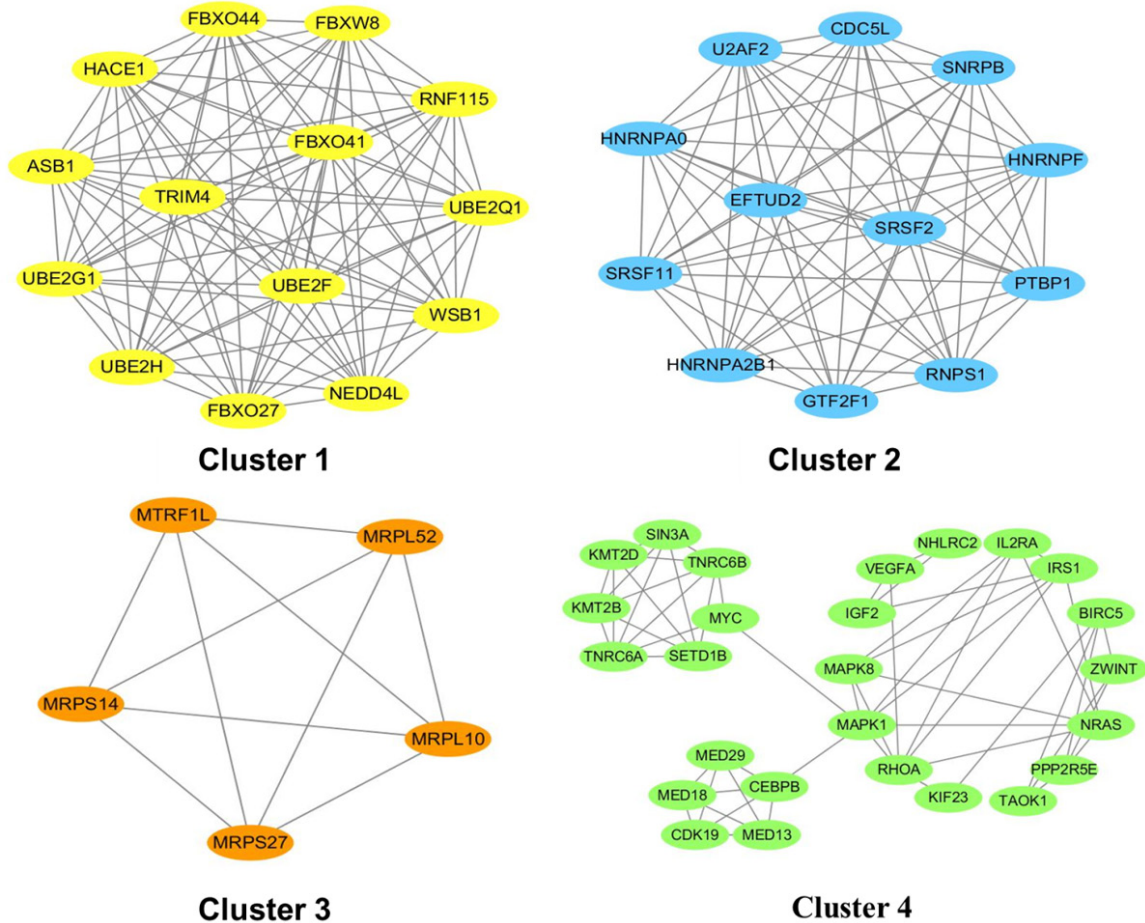
Figure 6. Top-4 module networks constructed by MCODE. The screening conditions were as follows: node score cutoff =0.2; K-score =2; maximum depth =100. MCODE, Molecular Complex Detection.

Table 7. List of the module genes and their overlap with the top-20 hub genes

Clusters	Gene symbol	Overlap with top-20 hub genes	Proportion
1	UBE2H, UBE2Q1, FBXO27, ASB1, RNF115, UBE2G1, WSB1, FBXO41, NEDD4L, TRIM4, FBXW8, FBXO44, HACE1, UBE2F	NEDD4L, FBXO44, FBXO27, WSB1, FBXW8, UBE2F, ASB1	35%
2	SRSF11, CDC5L, U2AF2, GTF2F1, RNPS1, SNRPB, PTBP1, SRSF2, HNRNPA0, HNRNPA2B1, HNRNPF, EFTUD2	RNPS1, CDC5L, SNRPB, U2AF2, GTF2F1, SRSF2	30%
3	MRPS27, MRPL10, MTRF1L, MRPS14, MRPL52	/	0%
4	IGF2, BIRC5, TNRC6B, KMT2D, KIF23, ZWINT, CEBPB, CDK19, SIN3A, MED29, IRS1, SETD1B, NRAS, IL2RA, KMT2B, MED18, NHLRC2, MYC, TNRC6A, MED13, MAPK1, MAPK8, VEGFA, PPP2R5E, RHOA, TAOK1	NRAS, MAPK1, TNRC6A, RHOA	8%

cers [45, 46]. A study conducted by Weihua Zhou et al. indicated that Neddylation E2 UBE2F promoted the survival of lung cancer cells by activating CRL5 to degrade NOXA via the K_{11} linkage [47]. Regarding ABS1, its differential methylation in ischemic cardiomyopathy was assessed by the relationship with left ventricular performance in end-stage heart failure patients [48]. However, few reports have investigated the relationship between these seven

hub genes and atherosclerosis. Therefore, this work is the first to convey the possibility of seven hub genes (NEDD4L, FBXO44, FBXO27, WSB1, FBXW8, UBE2F, and ASB1) associated with atherosclerosis.

In conclusion, this study identified macrophage circRNA hsa_circ_0005699 as being associated with atherosclerosis and its possible related function genes. This work might provide a
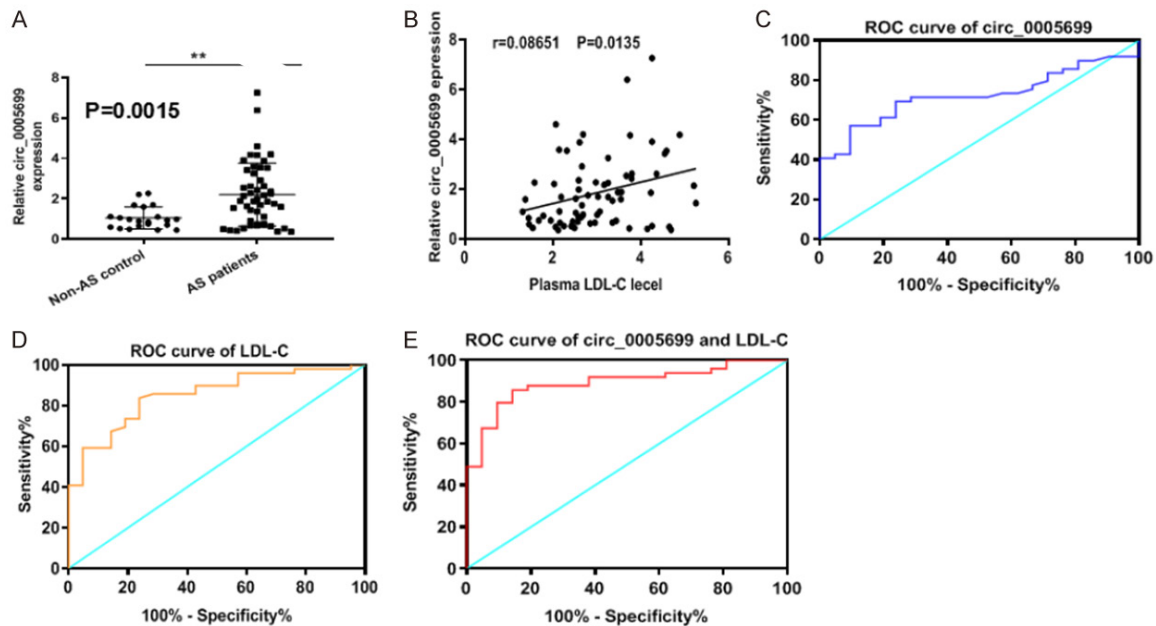
Figure 7. Correlation of hsa_circ_0005699 in plasma and LDL-C level with cerebral atherosclerosis. A. The expression of hsa_circ_0005699 as determined by qRT-PCR was increased in plasma from patients with atherosclerosis. B. Spearman correlation coefficients between hsa_circ_0005699 and LDL-C level. C. ROC analysis for hsa_circ_0005699 in the plasma for cerebral atherosclerosis. D. ROC of LDL-C for cerebral atherosclerosis. E. ROC of combination of hsa_circ_0005699 and LDL-C for cerebral atherosclerosis.

promising diagnostic biomarker and potentially effective drugs for atherosclerosis. However, the possible molecular mechanism of hsa_circ_0005699 in the development of atherosclerosis remains to be explored, such as validation of the expression analysis of relevant genes, histology analysis, and immunohistochemistry assay in atherosclerosis. Additionally, the functions of hsa_circ_0005699 and these molecular compounds in atherosclerosis need further experimental verification.

Acknowledgements

Disclosure of conflict of interest

None.

Address correspondence to: Yun Zhang, General Department of Medicine, Affiliated Hospital of Inner Mongolia Medical University, No. 1, Tongdao North Road, Huimin District, Hohhot 010050, The Inner Mongolia Autonomous Region, P. R. China. Tel: +86-15247128665; E-mail: 1056370989@qq.com

References

[1] Benjamin EJ, Muntner P, Alonso A, Bittencourt MS, Callaway CW, Carson AP, Chamberlain AM, Chang AR, Cheng S, Das SR, Delling FN, Djousse L, Elkind MSV, Ferguson JF, Fornage M, Jordan LC, Khan SS, Kissela BM, Knutson KL, Kwan TW, Lackland DT, Lewis TT, Lichtman JH, Longenecker CT, Loop MS, Lutsey PL, Martin SS, Matsushita K, Moran AE, Mussolino ME, O'Flaherty M, Pandey A, Perak AM, Rosamond WD, Roth GA, Sampson UKA, Satou GM, Schroeder EB, Shah SH, Spartano NL, Stokes A, Tirschwell DL, Tsao CW, Turakhia MP, VanWagner LB, Wilkins JT, Wong SS and Virani SS; American Heart Association Council on Epidemiology and Prevention Statistics Committee and Stroke Statistics Subcommittee. Heart disease and stroke statistics-2019 update: a report from the American Heart Association. Circulation 2019; 139: e56-e528.

[2] Frostegard J. Immunity, atherosclerosis and cardiovascular disease. BMC Med 2013; 11: 117.

[3]   Ross R. Atherosclerosis--an inflammatory disease. N Engl J Med 1999; 340: 115-126.

[4]   Frostegard J, Nilsson J, Haegerstrand A, Hamsten A, Wigzell H and Gidlund M. Oxidized low density lipoprotein induces differentiation and adhesion of human monocytes and the monocytic cell line U937. Proc Natl Acad Sci U S A 1990; 87: 904-908.

[5]   Chen LL. The biogenesis and emerging roles of circular RNAs. Nat Rev Mol Cell Biol 2016; 17: 205-211.

[6]   Memczak S, Jens M, Elefsinioti A, Torti F, Krueger J, Rybak A, Maier L, Mackowiak SD, Gregersen LH, Munschauer M, Loewer A, Ziebold U, Landthaler M, Kocks C, le Noble F and Rajewsky N. Circular RNAs are a large class of animal RNAs with regulatory potency. Nature 2013; 495: 333-338.

[7]   Lee SM, Kong HG and Ryu CM. Are circular RNAs new kids on the block? Trends Plant Sci 2017; 22: 357-360.

[8]   Devaux Y, Creemers EE, Boon RA, Werfel S, Thum T, Engelhardt S, Dimmeler S and Squire I. Circular RNAs in heart failure. Eur J Heart Fail 2017; 19: 701-709.

[9]   Han D, Li J, Wang H, Su X, Hou J, Gu Y, Qian C, Lin Y, Liu X, Huang M, Li N, Zhou W, Yu Y and Cao X. Circular RNA circMTO1 acts as the sponge of microRNA-9 to suppress hepatocellular carcinoma progression. Hepatology 2017; 66: 1151-1164.

[10] Zeng K, He B, Yang BB, Xu T, Chen X, Xu M, Liu X, Sun H, Pan Y and Wang S. The pro-metastasis effect of circANKS1B in breast cancer. Mol Cancer 2018; 17: 160.

[11] Wang K, Long B, Liu F, Wang JX, Liu CY, Zhao B, Zhou LY, Sun T, Wang M, Yu T, Gong Y, Liu J, Dong YH, Li N and Li PF. A circular RNA protects the heart from pathological hypertrophy and heart failure by targeting miR-223. Eur Heart J 2016; 37: 2602-2611.

[12] Barrett T, Troup DB, Wilhite SE, Ledoux P, Evangelista C, Kim IF, Tomashevsky M, Marshall KA, Phillippy KH, Sherman PM, Muertter RN, Holko M, Ayanbule O, Yefanov A and Soboleva A. NCBI GEO: archive for functional genomics data sets--10 years on. Nucleic Acids Res 2011; 39: D1005-1010.

[13] Glazar P, Papavasileiou P and Rajewsky N. circBase: a database for circular RNAs. RNA 2014; 20: 1666-1670.

[14] Li S, Li Y, Chen B, Zhao J, Yu S, Tang Y, Zheng Q, Li Y, Wang P, He X and Huang S. exoRBase: a database of circRNA, lncRNA and mRNA in human blood exosomes. Nucleic Acids Res 2018; 46: D106-D112.

[15] Xia S, Feng J, Chen K, Ma Y, Gong J, Cai F, Jin Y, Gao Y, Xia L, Chang H, Wei L, Han L and He C. CSCD: a database for cancer-specific circular RNAs. Nucleic Acids Res 2018; 46: D925-D929.

[16] Dudekula DB, Panda AC, Grammatikakis I, De S, Abdelmohsen K and Gorospe M. CircInteractome: a web tool for exploring circular RNAs and their interacting proteins and microRNAs. RNA Biol 2016; 13: 34-42.

[17] Li JH, Liu S, Zhou H, Qu LH and Yang JH. starBase v2.0: decoding miRNA-ceRNA, miRNA-ncRNA and protein-RNA interaction networks from large-scale CLIP-Seq data. Nucleic Acids Res 2014; 42: D92-97.

[18] Wang X. miRDB: a microRNA target prediction and functional annotation database with a wiki interface. RNA 2008; 14: 1012-1017.

[19] Hsu SD, Lin FM, Wu WY, Liang C, Huang WC, Chan WL, Tsai WT, Chen GZ, Lee CJ, Chiu CM, Chien CH, Wu MC, Huang CY, Tsou AP and Huang HD. miRTarBase: a database curates experimentally validated microRNA-target interactions. Nucleic Acids Res 2011; 39: D163-169.

[20] Szklarczyk D, Franceschini A, Wyder S, Forslund K, Heller D, Huerta-Cepas J, Simonovic M, Roth A, Santos A, Tsafou KP, Kuhn M, Bork P, Jensen LJ and von Mering C. STRING v10: protein-protein interaction networks, integrated over the tree of life. Nucleic Acids Res 2015; 43: D447-452.

[21] Shannon P, Markiel A, Ozier O, Baliga NS, Wang JT, Ramage D, Amin N, Schwikowski B and Ideker T. Cytoscape: a software environment for integrated models of biomolecular interaction networks. Genome Res 2003; 13: 2498-2504.

[22] Chin CH, Chen SH, Wu HH, Ho CW, Ko MT and Lin CY. cytoHubba: identifying hub objects and sub-networks from complex interactome. BMC Syst Biol 2014; 8 Suppl 4: S11.

[23] Dennis G Jr, Sherman BT, Hosack DA, Yang J, Gao W, Lane HC and Lempicki RA. DAVID: database for annotation, visualization, and integrated discovery. Genome Biol 2003; 4: P3.

[24] Chen EY, Tan CM, Kou Y, Duan Q, Wang Z, Meirelles GV, Clark NR and Ma'ayan A. Enrichr: interactive and collaborative HTML5 gene list enrichment analysis tool. BMC Bioinformatics 2013; 14: 128.

[25] Bader GD and Hogue CW. An automated method for finding molecular complexes in large protein interaction networks. BMC Bioinformatics 2003; 4: 2.

[26] Lukong KE, Chang KW, Khandjian EW and Richard S. RNA-binding proteins in human genetic disease. Trends Genet 2008; 24: 416-425.

[27] Rupaimoole R, Calin GA, Lopez-Berestein G and Sood AK. miRNA deregulation in cancer cells and the tumor microenvironment. Cancer Discov 2016; 6: 235-246.

[28] Frostegard J, Ulfgren AK, Nyberg P, Hedin U, Swedenborg J, Andersson U and Hansson GK. Cytokine expression in advanced human ath-

erosclerotic plaques: dominance of pro-inflammatory (Th1) and macrophage-stimulating cytokines. Atherosclerosis 1999; 145: 33-43.

[29] Greaves DR and Gordon S. Immunity, atherosclerosis and cardiovascular disease. Trends Immunol 2001; 22: 180-181.

[30] Tan S, Sun D, Pu W, Gou Q, Guo C, Gong Y, Li J, Wei YQ, Liu L, Zhao Y and Peng Y. Circular RNA F-circEA-2a derived from EML4-ALK fusion gene promotes cell migration and invasion in non-small cell lung cancer. Mol Cancer 2018; 17: 138.

[31] Hsiao KY, Lin YC, Gupta SK, Chang N, Yen L, Sun HS and Tsai SJ. Noncoding effects of circular RNA CCDC66 promote colon cancer growth and metastasis. Cancer Res 2017; 77: 2339-2350.

[32] Wang Y, Liu J, Ma J, Sun T, Zhou Q, Wang W, Wang G, Wu P, Wang H, Jiang L, Yuan W, Sun Z and Ming L. Exosomal circRNAs: biogenesis, effect and application in human diseases. Mol Cancer 2019; 18: 116.

[33] Zhang X, Wang S, Wang H, Cao J, Huang X, Chen Z, Xu P, Sun G, Xu J, Lv J and Xu Z. Circular RNA circNRIP1 acts as a microRNA-149-5p sponge to promote gastric cancer progression via the AKT1/mTOR pathway. Mol Cancer 2019; 18: 20.

[34] Zhu YJ, Zheng B, Luo GJ, Ma XK, Lu XY, Lin XM, Yang S, Zhao Q, Wu T, Li ZX, Liu XL, Wu R, Liu JF, Ge Y, Yang L, Wang HY and Chen L. Circular RNAs negatively regulate cancer stem cells by physically binding FMRP against CCAR1 complex in hepatocellular carcinoma. Theranostics 2019; 9: 3526-3540.

[35] Salmena L, Poliseno L, Tay Y, Kats L and Pandolfi PP. A ceRNA hypothesis: the Rosetta Stone of a hidden RNA language? Cell 2011; 146: 353-358.

[36] Cheng Z, Yu C, Cui S, Wang H, Jin H, Wang C, Li B, Qin M, Yang C, He J, Zuo Q, Wang S, Liu J, Ye W, Lv Y, Zhao F, Yao M, Jiang L and Qin W. circTP63 functions as a ceRNA to promote lung squamous cell carcinoma progression by up-regulating FOXM1. Nat Commun 2019; 10: 3200.

[37] Chen L, Nan A, Zhang N, Jia Y, Li X, Ling Y, Dai J, Zhang S, Yang Q, Yi Y and Jiang Y. Circular RNA 100146 functions as an oncogene through direct binding to miR-361-3p and miR-615-5p in non-small cell lung cancer. Mol Cancer 2019; 18: 13.

[38] Dahlberg J, Sjögren M, Hedblad B, Engström G and Melander O. Genetic variation in NEDD4L, an epithelial sodium channel regulator, is associated with cardiovascular disease and cardiovascular death. J Hypertens 2014; 32: 294-299.

[39] He S, Deng J, Li G, Wang B, Cao Y and Tu Y. Down-regulation of Nedd4L is associated with the aggressive progression and worse prognosis of malignant glioma. Jpn J Clin Oncol 2012; 42: 196-201.

[40] Sjögren B, Swaney S and Neubig RR. FBXO44-mediated degradation of RGS2 protein uniquely depends on a cullin 4B/DDB1 complex. PLoS One 2015; 10: e0123581.

[41] Yoshida Y, Yasuda S, Fujita T, Hamasaki M, Murakami A, Kawawaki J, Iwai K, Saeki Y, Yoshimori T, Matsuda N and Tanaka K. Ubiquitination of exposed glycoproteins by SCF(FBXO27) directs damaged lysosomes for autophagy. Proc Natl Acad Sci U S A 2017; 114: 8574-8579.

[42] Yao RQ, Ren C, Xia ZF and Yao YM. Organelle-specific autophagy in inflammatory diseases: a potential therapeutic target underlying the quality control of multiple organelles. Autophagy 2021; 17: 385-401.

[43] Jia YY, Zhao JY, Li BL, Gao K, Song Y, Liu MY, Yang XJ, Xue Y, Wen AD and Shi L. miR-592/WSB1/HIF-1α axis inhibits glycolytic metabolism to decrease hepatocellular carcinoma growth. Oncotarget 2016; 7: 35257-35269.

[44] Cao J, Wang Y, Dong R, Lin G, Zhang N, Wang J, Lin N, Gu Y, Ding L, Ying M, He Q and Yang B. Hypoxia-induced WSB1 promotes the metastatic potential of osteosarcoma cells. Cancer Res 2015; 75: 4839-4851.

[45] Pan ZQ. Cullin-RING E3 ubiquitin ligase 7 in growth control and cancer. Adv Exp Med Biol 2020; 1217: 285-296.

[46] Wang J, Bogdanova N, Schürmann P, Park-Simon TW, Geffers R and Dörk T. Assessment of a FBXW8 frameshift mutation, c.1312_1313delGT, in breast cancer patients and controls from Central Europe. Cancer Genet 2018; 220: 38-43.

[47] Zhou W, Xu J, Li H, Xu M, Chen ZJ, Wei W, Pan Z and Sun Y. Neddylation E2 UBE2F promotes the survival of lung cancer cells by activating CRL5 to degrade NOXA via the K11 linkage. Clin Cancer Res 2017; 23: 1104-1116.

[48] Ortega A, Tarazón E, Gil-Cayuela C, Martínez-Dolz L, Lago F, González-Juanatey JR, Sandoval J, Portolés M, Roselló-Lletí E and Rivera M. ASB1 differential methylation in ischaemic cardiomyopathy: relationship with left ventricular performance in end-stage heart failure patients. ESC Heart Fail 2018; 5: 732-737.